Supplementary Information (SI) for Journal of Materials Chemistry C.
This journal is © The Royal Society of Chemistry 2024

Supplementary Data

Effective Strategies for Current Boosting in a Mesa-Shaped In-Ga-Zn-O Vertical-Channel Thin-Film Transistors with a Short-Channel Length of 40 nm

Chae-Eun Oh[1], Young-Ha Kwon[2], Nak-Jin Seong[2], Kyu-Jeong Choi[2], Sung-Min Yoon*[1]

[1]Department of Advanced Materials Engineering for Information and Electronics,
Kyung Hee University, Yongin, Gyeonggi-do 17104, Korea.
[2]NCD Co., Ltd, Daejeon 34015, Korea.

*E-mail: sungmin@khu.ac.kr

1. Electrical separation between top and bottom ITO electrodes of mesa-shaped VCTs

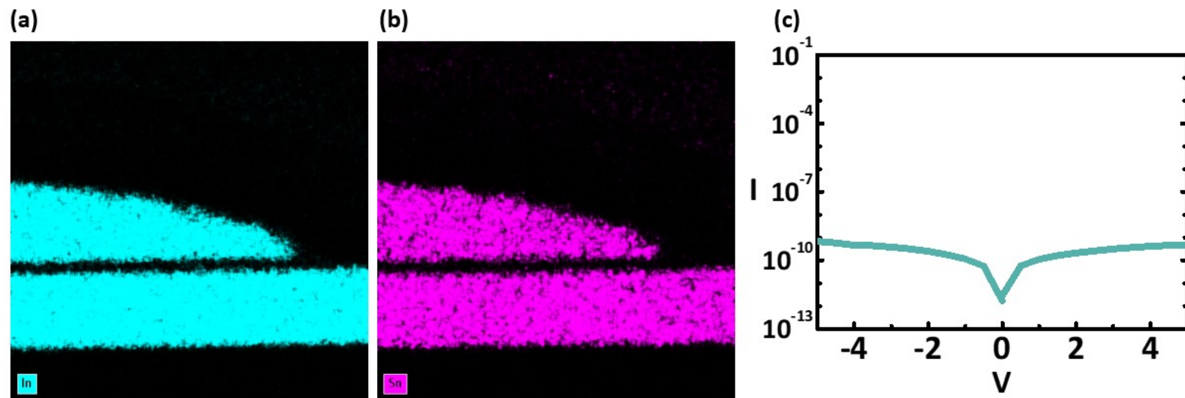

Figure S1. Energy-dispersive X-ray spectrometer (EDS) mapping images (a) In and (b) Sn in the Al_2O_3 spacer pattern intervening between the ITO source and drain electrode layers of the IGZO VCT with a channel length of 20 nm. (c) I-V Characteristics of the ITO/Al_2O_3 spacer (40 nm)/ITO structures in the IGZO VCT. The two components of In and Sn were clearly identified at the locations of the source and drain electrodes, thereby confirming that the top and bottom ITO electrodes were effectively separated, as shown in Figs. S1(a) and 1(b). This has also been confirmed for the IGZO VCTs with a channel length of 40 nm. Given that the drain and source electrodes are electrically connected, the VCT is susceptible to failure in its device operations. Figure S1(c) shows the I-V characteristics measured between the top and bottom electrodes after the spacer patterning process using a hybrid-etching technique, demonstrating that two electrodes were successfully isolated without the formation of any conducting paths.

2. Influence of field distribution in mesa-shaped IGZO VCTs

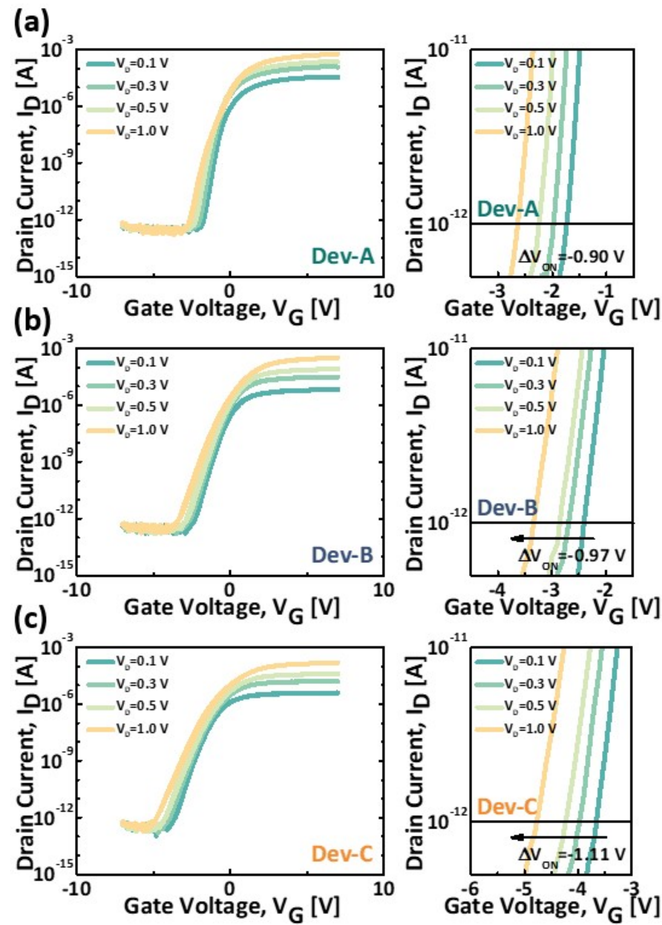

Figure S2. Variations in the transfer characteristics of the (a) Dev-A, (b) Dev-B, and (c) Dev-C, when the V_{DS} was applied to the bottom electrode within the range of 0.1 to 1.0 V, with the magnified views in transfer curves.

Table S1. Summary of the I_{DS} values, which were extracted from the transfer characteristics shown in Figs. 2a-c, when the V_{DS} was varied to 0.1, 0.3, 0.5, and 1.0 V.

	Drain voltage, V_{DS} [V]			
	0.1	0.3	0.5	1.0
Drain current, $I_{DS,Dev-A}$ [V]	7.4	22	35	65
Drain current, $I_{DS,Dev-B}$ [V]	0.87	5.2	13	45
Drain current, $I_{DS,Dev-C}$ [V]	0.75	4.4	12	41

Table S2. Summary of the ΔV_{ON} and λ_{DIBL} values for the fabricated devices when the V_{DS} was varied from 0.1 to 1.0 V.

	Dev-A	Dev-B	Dev-C
ΔV_{ON} [V]	- 0.9	- 0.97	- 1.11
λ_{DIBL} [mV/V]	100	107	123

The structural features of the mesa-shaped VCTs have the potential to influence the DIBL characteristics of the IGZO VCTs. In other words, in the VCTs implemented with mesa-shaped vertical sidewalls, large overlapping region between the vertical gate and the top drain electrode can be situated, including the edge area with a small curvature of radius in the vicinity of the top drain at the edge of the spacer pattern. Therefore, the application of a higher drain bias (V_{DS}) to the top drain electrode results in the concentration of the electric field at the drain edge, thereby inducing a higher lateral field [R1]. The impact of the lateral electric field is typically increased with a reduction in the L_{CH}, resulting in a further enhancement of the lateral field concentration at the drain edge for mesa-shaped VCTs with an L_{CH} as short as 40 nm [R2]. The impact of field concentration results in the generation of a larger number of conduction carriers in the vicinity of the top drain electrode, which may effectively suppress the DIBL effect by inhibiting the expansion of the depletion region as the increase in the V_{DS}.

The values of λ_{DIBL} were found to be intensified with increasing the T_{CH}. In other words, the λ_{DIBL} values were calculated to be 88 (Dev-B) and 122 mV/V (Dev-C) when the T_{CH} was varied from 10 to 15 nm. It seems reasonable to suggest that the impact of lateral field concentration can be influenced by modulating the T_{CH} for mesa-shaped VCTs. As the T_{CH} increases, the

rounding in the vicinity of the top drain at the edge of the spacer pattern can be mitigated, thereby reducing the gate controllability by spreading the concentrated field in comparison to the devices employing thinner T_{CH} [R3]. Furthermore, the incorporation of H into the front channel region can be more effectively facilitated through the reduction of T_{CH}. Consequently, the expansion of the depletion region from the drain electrode can be further suppressed, thereby improving the DIBL characteristics [R4]. Alternatively, the Dev-A exhibited a ΔV_{ON} of +0.11 V with the V_{DS} was varied from 0.1 to 1.0 V, resulting in a λ_{DIBL} of -116 mV/V. Thus, in order to accurately elucidate the DIBL phenomena for the fabricated IGZO VCTs, the variations in the drain current (I_{DS}) were compared with the increase in the V_{DS} between the devices. Table S1 summarizes the values of I_{DS}, which were extracted from the transfer characteristics shown in Figs. 2a-c at a gate voltage (V_G) of 7 V, when the V_{DS} was varied to 0.1, 0.3, 0.5, and 1.0 V. It is noteworthy that for the Dev-A, the obtained I_{DS} values exhibited a strong correlation with the current scaling with V_{DS}. In contrast, for the Dev-B and Dev-C, the values of I_{DS} were not proportionately increased as a consequence of the effects of DIBL and contact resistance. It can be concluded that, despite the absence of a severe level of DIBL in all fabricated devices, the reduction in the T_{CH} can be identified as a key strategy for the suppression of short-channel effects, including DIBL, in mesa-shaped VCTs. Furthermore, to clearly verify the impact of gate controllability on the DIBL, the device characteristics the Dev-AL, which corresponds to the controlled device fabricated with a thicker GI thickness of 40 nm, were also investigated. The values of ΔV_{ON} and the λ_{DIBL} were estimated to be -0.10 V and 111 mV/V, respectively. These values were found to be inferior to those obtained from the Dev-A and Dev-B, and be analogous to those obtained from the Dev-C. These results are in

accordance with the investigations described in the manuscript, which indicated that the gate controllability lost its effect due to the increase in natural length (λ, Dev-A: 11.5 nm, Dev-B: 16.2 nm, Dev-C: 19.9 nm, and Dev-AL: 17.2 nm) with increasing the GI thickness.

The supplementary measurements were conducted to assess the validity of the aforementioned discussions. In order to ascertain the impact of field concentration at the edge of the spacer pattern in the vicinity of the top drain, the DIBL characteristics were also evaluated using the bottom ITO electrode as a drain, as shown in Fig. S2. Figures S2(a)-(c) show the variations in the transfer characteristics of the Dev-A, Dev-B, and Dev-C, respectively, when the V_{DS} was applied to the bottom electrode within the range of 0.1 to 1.0 V, with the magnified views in transfer curves. Table S2 summarizes the values of ΔV_{ON} and λ_{DIBL} for the fabricated devices when the V_{DS} was varied from 0.1 to 1.0 V. It is noteworthy that all devices exhibited negative shifts in V_{ON} from the initial increase in V_{DS}. Furthermore, the values of ΔV_{ON} and λ_{DIBL} were more pronounced than those obtained when the top electrode was employed as a drain, resulting in a greater degree of the DIBL effect. These interesting findings suggest that the influences of field concentration and T_{CH} may have considerable impact on the overall device characteristics, including the DIBL, for the fabricated VCTs. It should be noted, however, that the process-related damage to the bottom electrode of the VCT may occur as a result of plasma etching during the spacer patterning process, which may play a dominant role in determining the device characteristics. This suggests that the effects of the field distribution, in conjunction with the effects of damaged ITO electrodes, are likely to be reflected in the results presented in Table S2 in a complex manner.

3. Device-to-device uniformity of the IGZO VCTs over variations in channel thickness

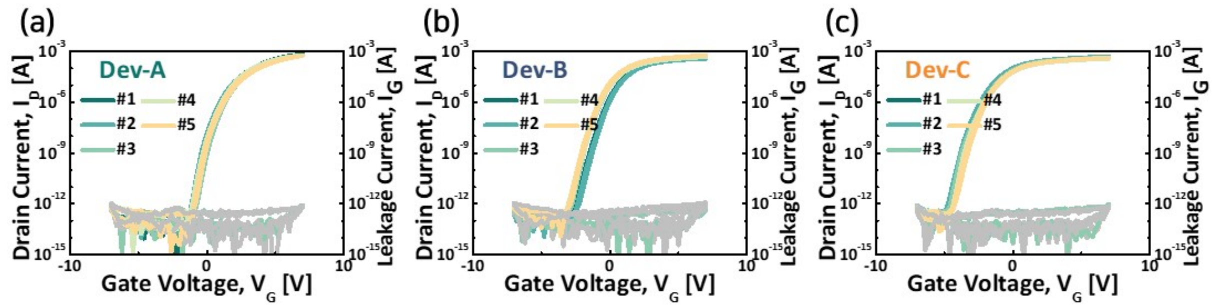

Figure S3. Comparisons in transfer curves collected from 5 devices of (a) Dev-A, (b) Dev-B, and (c) Dev-C in order to verify device-to-device uniformity. There were not any big differences in switching operations, including the turn-on voltages, among the devices in all cases. The results demonstrated that the standard deviations of each device parameter were sufficiently low, indicating that the fabricated IGZO VCTs with an L_{CH} of 40 nm exhibited an acceptable level of device uniformity and reproducibility. Furthermore, even when the T_{GI} was scaled down to 15 nm, all devices exhibited gate leakage current values of less than 1 pA.

4. PBTS stabilities of the devices with channel thickness variations

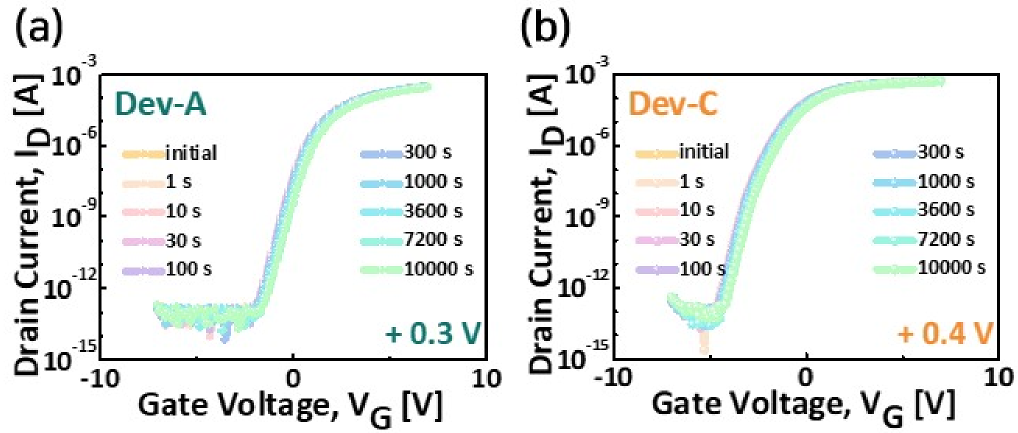

Figure S4. Variations in transfer curves with a lapse of stress time for 10^4s under the PBTS conditions at 60 °C for (a) Dev-A and (b) Dev-C, respectively. Transfer characteristics showed no significant difference in turn-on voltage over time for either device. This indicates that all the devices implemented using identical fabrication process conditions exhibited interfacial properties with an acceptable quality.

5. Process strategy for Al_2O_3 spacers to control the degree of H incorporated in IGZO VCTs

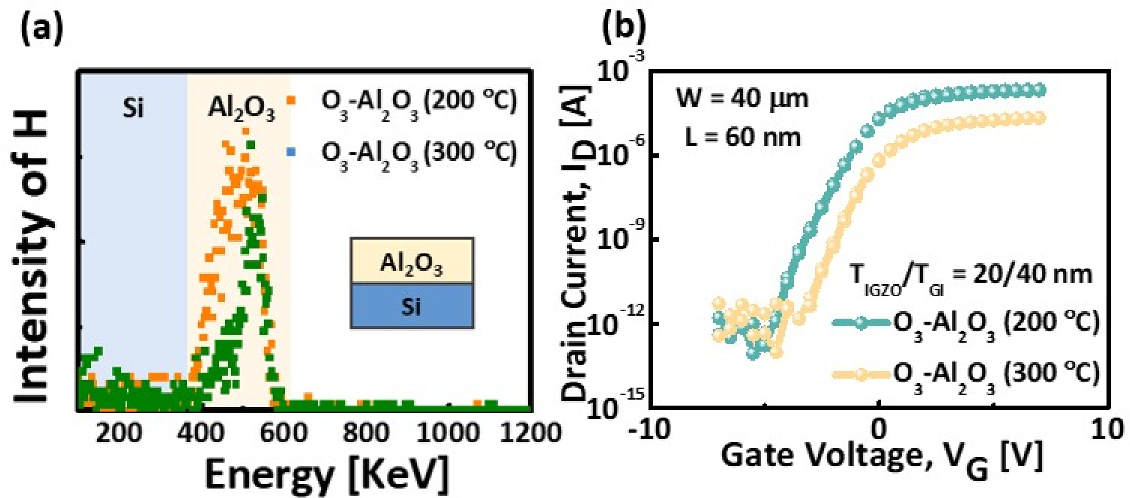

Figure S5. (a) ERD spectra in the RBS measurements for the ALD-Al_2O_3 films prepared with O_3 oxidant at different temperatures of 200 and 300 °C. (b) Comparisons in transfer characteristics of the IGZO VCTs (with a channel length of 60 nm) fabricated with O_3-Al_2O_3 spacer deposited at different temperatures. The most effective method for controlling the hydrogen content within the Al_2O_3 deposited by ALD is to modulate the deposition temperature. From the viewpoint of improvement in the C_{DR} for the devices using O_3-Al_2O_3 spacer, an initial investigation was conducted to ascertain the impact of deposition temperature on the devices using an Al_2O_3 spacer with a thickness of 60 nm. The incomplete reaction of the TMA precursor with the O_3 oxidant during the ALD process under low temperature conditions has the potential to result in the generation of OH radicals from the dangling bonds of Al_2O_3. The formation of radicals may also result in an increase in the hydrogen content within the Al_2O_3 layers. Figure S5(a) presents a comparative analysis of the hydrogen contents between the O_3-Al_2O_3 layers deposited at 200 and 300 °C. The hydrogen concentration in Al_2O_3 was estimated to decrease from 1.96 to 1.08 at% as the increase in

deposition temperature from 200 to 300 °C. Figure S5(b) compares the transfer characteristics of the IGZO VCTs fabricated using the Al_2O_3 spacers deposited at temperatures of 200 and 300 °C. It is noteworthy that the device using the O_3-Al_2O_3 spacer with a higher hydrogen content exhibited a higher C_{DR} (5.1 μA/μm) in comparison to the device using the O_3-Al_2O_3 spacer with a lower hydrogen content (0.05 μA/μm). According to these obtained results, it can be expected that the control of deposition temperature may also be an effective method for adjusting the hydrogen content in H_2O-Al_2O_3 layers.

References

[R1] X. Yin, S. Deng, G. Li, W. Zhong, R. Chen, G. Li, F. S. Y. Yeung, M. Wong, H. S. Kwok, Low Leakage Current Vertical Thin-Film Transistors With InSnO-Stabilized ZnO Channel, IEEE Electron Devices Letters, 2020, 41, 248-251, doi: 10.1109/LED.2019.2960883

[R2] Y. Li, Y.L. Pei, R.Q. Hu, Z.M. Chen, Y. Zhao, Z. Shen, B.F. Fan, J. Liang, G. Wang, Effect of channel thickness on electrical performance of amorphous IGZO thin-film transistor with atomic layer deposited alumina oxide dielectric, Current Applied Physics, 2014, 14, 941-945, doi: 10.1016/j.cap.2014.04.011

[R3] D. Kim, J.-H. Kim, W. S. Choi, T. J. Yang, J. T. Jang, A. Belmonte, N. Rassoul, S. Subhechha, R. Delhougne, G. S. Kar, W. Lee, M. H. Cho, D. Ha&D. H. Kim, Device modeling of two-steps oxygen anneal-based submicron InGaZnO back-end-of-line field-effect transistor enabling short-channel effects suppression, Scientific Reports, 2022, 12, p1-12, doi: 10.1038/s41598-022-23951-x

[R4] T. J. Yang, J.-H. Kim, J. R. Cho, H. J. Lee, K. Kim, J. Park, S.-J. Choi, J.-H. Bae, D. M. Kim, C. Kim, D.-W. Park, D. H. Kim, Physical model of a local threshold voltage shift in InGaZnO thin-film transistors under current stress for instability-aware circuit design, Current Applied Physics, 2023, 46, 55-60, doi: 10.1016/j.cap.2022.11.011